PERGAMON

International Journal of Solids and Structures 39 (2002) 5241–5251

INTERNATIONAL JOURNAL OF SOLIDS and STRUCTURES

www.elsevier.com/locate/ijsolstr

Rotation sensitivity of waves propagating in a rotating piezoelectric plate

H.Y. Fang [a], J.S. Yang [a], Q. Jiang [b,*]

[a] *Department of Engineering Mechanics, University of Nebraska, Lincoln, NE 68588, USA*
[b] *Department of Mechanical Engineering, University of California, Riverside, CA 92521-0425, USA*

Received 20 November 2001; received in revised form 15 May 2002

Abstract

The rotation effect on the characteristics of waves propagating in a piezoelectric plate is studied in the framework of linear piezoelectricity including Coriolis and centrifugal forces. The rotation sensitivity of the wave dispersion relations is analyzed in details for polarized ceramic plates and for the lowest thickness-shear and the lowest thickness-twist waves because of the particular importance of these modes for gyroscope applications. The analysis shows that the frequency shifts monotonically with the increasing rotation rate and the rotation sensitivity of long waves is substantially greater than that of short waves. Generally, plates with shorted electrode surfaces have higher rotation sensitivity than plates with free-charge surfaces. For long waves and for small rotation rate relative to the wave frequency, the frequency shifts with rotation rate, linearly for plates with shorted electrode surfaces and nonlinearly with a nearly flat initial tangent for plates with free-charge surfaces. These rotation sensitivity characteristics are of interest for the development of rotation sensors and other piezoelectric devices for which frequency insensitivity to rotation is desired.

Keywords: Acoustic waves; Piezoelectrics; Sensors; Gyroscopes

1. Introduction

Characteristics of waves propagating in solids and their dependence upon various geometric and physical parameters have been under continued study. The effects of pre-stress, acceleration, and temperature variation, etc., on wave speed or frequency provide the foundation for the development of many acoustic sensors (White, 1998). Particularly, frequency shifts due to rotation have been used to make gyroscopes, i.e., angular rate sensors, see Tiersten et al. (1980, 1981), Lao (1980), Clarke and Burdess (1994), and Yang et al. (1988) for example. These sensors may operate with bulk waves in plates and rings (Tiersten et al., 1981; Yang et al., 1988), or surface waves over a half-space (Tiersten et al., 1980; Lao, 1980; Clarke

* Corresponding author. Tel.: +1-909-787-5190; fax: +1-909-787-3188.
E-mail address: qjiang@engr.ucr.edu (Q. Jiang).

0020-7683/02/$ - see front matter © 2002 Elsevier Science Ltd. All rights reserved.
PII: S0020-7683(02)00375-X

and Burdess, 1994). For sensor applications, frequency shifts need to be maximized through design for high sensitivity. On the other hand, there are many resonant piezoelectric devices, such as those mounted on moving objects for timing and frequency control, for which a stable working frequency *insensitive* to motion or other changes in the working environment is desired, as investigated by Tiersten and Shick (1988) and Shick et al. (1989). The development of such devices requires the understanding of the mechanical characteristics of rotating piezoelectric bodies, for the purpose of either making use of the rotation-induced frequency shift or avoiding it. The present study focuses on the rotation effect upon waves propagation in piezoelectric plates.

Propagation of waves in piezoelectric plates has been an active research subject for several decades because of the applications in piezoelectric transducers, resonators, filters and other devices. A number of exact solutions of the three-dimensional dynamic equations have been obtained for widely used materials, such as polarized ceramics (Tiersten, 1963a,b; Onoe et al., 1963; Bleustein, 1969), various crystal cuts of quartz (Tiersten, 1963a; Schmidt, 1977a,b), and materials of other symmetries (Paul and Renganathan, 1985; Paul and Raman, 1991; Stewart and Yong, 1994). These solutions include thickness vibrations (Tiersten, 1963a; Onoe et al., 1963) and waves propagating within the plane of the plate (Tiersten, 1963b; Bleustein, 1969; Paul, 1968; Paul et al., 1983; Schmidt, 1977a,b; Syngellakis and Lee, 1993). From the viewpoint of the three-dimensional theory, thickness vibration modes of a plate can be viewed as waves propagating along the thickness direction of the plate and are bounced back and forth between the two major faces of the plate, with the wave vector parallel to the thickness direction. These thickness waves or vibration modes can exist only in infinite plates theoretically, and they are the idealized working modes of many resonant piezoelectric devices. In reality, due to the finite size of a plate-like device, pure thickness modes are not possible and the working modes of these devices are in fact related to three-dimensional waves propagating slightly off the thickness direction of the plate, for which the wave vector has a small component within the plane of the plate, called the in-plane or transverse component. These waves have been referred to as essentially thickness waves, or transversely varying thickness waves. On the other hand, from the viewpoint of the plate model, they are long waves propagating within the plane of the plate, with the in-plane wavelength much larger than the plate thickness. Understanding of the long waves is important for piezoelectric plate device applications. For instance, the in-plane wavelength is closely related to the dimensions of a plate device, and the frequency is essentially determined by the plate thickness.

Pure thickness vibration of a piezoelectric plate rotating about its normal at a constant rate has been studied in Bleustein (1968) from the viewpoint of the three-dimensional theory. To study the rotation effect upon the characteristics of waves propagating within the plane of a piezoelectric plate, we present in this paper a theoretical analysis on waves propagating in a piezoelectric plate that rotates about its normal at a constant angular rate. We begin in Section 2 with a general formulation of this phenomenon for piezoelectric materials of general material anisotropy. We then present in Section 3 a solution procedure leading to the frequency equation that determines the frequencies of various waves propagating in a piezoelectric plate rotating about its normal at a constant rate. We devote Section 4 to the solutions of the frequency equation for polarized ceramics and the implications of these solutions concerned with the rotation effect upon the characteristics of the plate waves.

2. Formulation of the problem

Consider an unbounded piezoelectric plate of thickness $2h$, rotating at a constant angular rate Ω about its normal, as schematically illustrated in Fig. 1. The plate is assumed to undergo small amplitude vibrations in the system of Cartesian coordinates x_i, attached to the rotating plate, with the x_2 axis along the normal of the plate. The dynamic equations of linear piezoelectricity (Tiersten, 1969) with Coriolis and centrifugal forces take the following form in this coordinate system:

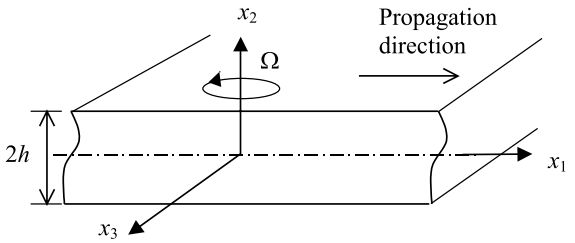

Fig. 1. Schematic illustration of a piezoelectric plate rotating about its normal.

$$c_{ijkl}u_{k,jl} + e_{kij}\phi_{,jk} = \rho[\ddot{u}_i + 2\varepsilon_{ijk}\Omega_j\dot{u}_k + (\Omega_i\Omega_j u_j - \Omega_j\Omega_j u_i)], \quad e_{ijk}u_{j,ik} - \varepsilon_{ij}\phi_{,ij} = 0, \tag{2.1}$$

where $(\Omega_1, \Omega_2, \Omega_3) = (0, \Omega, 0)$, and we denote by u_i the mechanical displacements and by ϕ the electric potential. c_{ijkl}, e_{kij} and ε_{ij} stand for the elastic, piezoelectric and dielectric constants, and ρ for the mass density, respectively. The summation convention for repeated tensor indices and the convention that a comma followed by an index denotes partial differentiation with respect to the coordinate associated with the index are adopted. The indices i, j, k, and l are ranged from 1 to 3. A superimposed dot represents time derivative. With the compressed matrix notation (Tiersten, 1969), the material constants c_{ijkl} and e_{ijk} in (2.1) can be represented by matrices c_{pq} and e_{ip}, with the convention that $p, q = 1, \ldots, 6$. Similarly, the strain tensor S_{ij} and the stress tensor T_{ij} can be represented by S_p and T_q. Over the major surfaces of the plate ($x_2 = \pm$h), the following traction-free mechanical boundary conditions are always assumed

$$T_{2j}(\pm h) = [c_{2jkl}u_{k,l} + e_{k2j}\phi_{,k}]_{x_2=\pm h} = 0, \tag{2.2}$$

where the linear piezoelectric constitutive relations (Tiersten, 1969) have been used. The commonly used electrical boundary conditions on the plate surfaces are a pair of shorted and grounded electrodes for which

$$\phi(h) = \phi(-h) = 0, \tag{2.3}$$

or a pair of unelectroded and charge-free surfaces for which

$$D_2(\pm h) = [e_{2jk}u_{j,k} - \varepsilon_{2j}\phi_{,j}]_{x_2=\pm h} = 0. \tag{2.4}$$

For an unelectroded surface, the effect of the electric field in the surrounding space can be considered by requiring that both the electrical potential and the normal component D_2 of the dielectric displacement vector cross the interface continuously. In the present discussion, the electrodes are assumed to be so thin that their mechanical effects can be neglected. The above equations and boundary conditions are homogeneous, and constitute an eigenvalue problem. We consider straight-crested waves propagating in the x_1 direction with $\partial/\partial x_3 = 0$. Then (2.1) assumes the following form

$$\begin{aligned}
&c_{11}u_{1,11} + c_{12}u_{2,21} + c_{14}u_{3,21} + c_{15}u_{3,11} + c_{16}(u_{1,21} + u_{2,11}) + e_{11}\phi_{,11} + e_{21}\phi_{,21} + c_{16}u_{1,12}\\
&\quad + c_{26}u_{2,22} + c_{46}u_{3,22} + c_{56}u_{3,12} + c_{66}(u_{1,22} + u_{2,12}) + e_{16}\phi_{,12} + e_{26}\phi_{,22} = \rho\ddot{u}_1 + 2\rho\Omega\dot{u}_3 - \rho\Omega^2 u_1,\\
&c_{16}u_{1,11} + c_{26}u_{2,21} + c_{46}u_{3,21} + c_{56}u_{3,11} + c_{66}(u_{1,21} + u_{2,11}) + e_{16}\phi_{,11} + e_{26}\phi_{,21}\\
&\quad + c_{12}u_{1,12} + c_{22}u_{2,22} + c_{24}u_{3,22} + c_{25}u_{3,12} + c_{26}(u_{1,22} + u_{2,12}) + e_{12}\phi_{,12} + e_{22}\phi_{,22} = \rho\ddot{u}_2,\\
&c_{15}u_{1,11} + c_{25}u_{2,21} + c_{45}u_{3,21} + c_{55}u_{3,11} + c_{56}(u_{1,21} + u_{2,11}) + e_{15}\phi_{,11} + e_{25}\phi_{,21} + c_{14}u_{1,12}\\
&\quad + c_{24}u_{2,22} + c_{44}u_{3,22} + c_{45}u_{3,12} + c_{46}(u_{1,22} + u_{2,12}) + e_{14}\phi_{,12} + e_{24}\phi_{,22} = \rho\ddot{u}_3 - 2\rho\Omega\dot{u}_1 - \Omega^2 u_3,\\
&e_{11}u_{1,11} + e_{12}u_{2,21} + e_{14}u_{3,21} + e_{15}u_{3,11} + e_{16}(u_{1,21} + u_{2,11}) - \varepsilon_{11}\phi_{,11} - \varepsilon_{12}\phi_{,21}\\
&\quad + e_{21}u_{1,12} + e_{22}u_{2,22} + e_{24}u_{3,22} + e_{25}u_{3,12} + e_{26}(u_{1,22} + u_{2,12}) - \varepsilon_{12}\phi_{,12} - \varepsilon_{22}\phi_{,22} = 0.
\end{aligned} \tag{2.5}$$

The boundary conditions (2.2)–(2.4) also take simpler forms correspondingly.

3. Solution procedure

We seek solutions in the following form:

$$\begin{aligned} u_j(\mathbf{x},t) &= A_j e^{k\eta x_2} e^{i(kx_1-\omega t)}, \\ \phi(\mathbf{x},t) &= A_4 e^{k\eta x_2} e^{i(kx_1-\omega t)}, \end{aligned} \tag{3.1}$$

where k and ω are the wave number in the x_1 direction and the time frequency, respectively. ηk is related to the wave number in the x_2 direction. A_j ($j=1,2,3$) and A_4 are complex constants, representing the wave amplitude. The complex notation is adopted with the real parts representing the physical quantities of interest. Substitution of (3.1) into (2.5) leads to the following four linear algebraic equations for A_j and A_4:

$$\begin{aligned} &[\rho(\omega^2+\Omega^2)+k^2(\eta^2 c_{66}+i2\eta c_{16}-c_{11})]A_1+k^2(\eta^2 c_{26}+i\eta c_{66}+i\eta c_{12}-c_{16})A_2 \\ &\quad+[\rho i2\Omega\omega+k^2(\eta^2 c_{46}+i\eta c_{56}+i\eta c_{14}-c_{15})]A_3+k^2(\eta^2 e_{26}+i\eta e_{21}+i\eta e_{16}-e_{11})A_4=0, \\ &k^2(\eta^2 c_{26}+i\eta c_{21}+i\eta c_{66}-c_{16})A_1+[\rho\omega^2+k^2(\eta^2 c_{22}+i2\eta c_{26}-c_{66})]A_2 \\ &\quad+k^2(\eta^2 c_{24}+i\eta c_{25}+i\eta c_{46}-c_{56})A_3+k^2(\eta^2 e_{22}+i\eta e_{26}+i\eta e_{12}-e_{16})A_4=0, \\ &[-\rho i2\Omega\omega+k^2(\eta^2 c_{46}+i\eta c_{14}+i\eta c_{56}-c_{15})]A_1+k^2(\eta^2 c_{24}+i\eta c_{46}+i\eta c_{25}-c_{56})A_2 \\ &\quad+[\rho(\omega^2+\Omega^2)+k^2(\eta^2 c_{44}+i2\eta c_{45}-c_{55})]A_3+k^2(\eta^2 e_{24}+i\eta e_{25}+i\eta e_{14}-e_{15})A_4=0, \\ &(\eta^2 e_{26}+i\eta e_{21}+i\eta e_{16}-e_{11})A_1+(\eta^2 e_{22}+i\eta e_{26}+i\eta e_{12}-e_{16})A_2 \\ &\quad+(\eta^2 e_{24}+i\eta e_{25}+i\eta e_{14}-e_{15})A_3-(\eta^2\varepsilon_{22}+i2\eta\varepsilon_{12}-\varepsilon_{11})A_4=0. \end{aligned} \tag{3.2}$$

For nontrivial solutions of A_j and/or A_4, the determinant of the coefficient matrix of the above equations must vanish, and this leads to a polynomial equation of degree eight for η. The coefficients of this polynomial equation are generally complex. We denote the eight roots by $\eta_{(m)}$, and the corresponding eigenvectors by $(\overline{A}_j^{(m)}, \overline{A}_4^{(m)})$, $m=1,2,\ldots,8$. Thus, the general wave solution to (2.5) in the form of (3.1) can be written as

$$u_i=\sum_{m=1}^{8} C_{(m)}\overline{A}_i^{(m)} e^{k\eta_{(m)}x_2} e^{i(kx_1-\omega t)}, \qquad \phi=\sum_{m=1}^{8} C_{(m)}\overline{A}_4^{(m)} e^{k\eta_{(m)}x_2} e^{i(kx_1-\omega t)}, \tag{3.3}$$

where the constants $C_{(m)}$ ($m=1,2,\ldots,8$) are to be determined. Substituting (3.3) into the boundary conditions (2.2) and (2.4) yields the following eight linear algebraic equations for $C_{(m)}$

$$\sum_{m=1}^{8}\left(c_{12}i\overline{A}_1^{(m)}+c_{22}\eta_{(m)}\overline{A}_2^{(m)}+c_{24}\eta_{(m)}\overline{A}_3^{(m)}+c_{25}i\overline{A}_3^{(m)}+c_{26}\eta_{(m)}\overline{A}_1^{(m)}+c_{26}i\overline{A}_2^{(m)}+e_{12}i\overline{A}_4^{(m)}+e_{22}\eta_{(m)}\overline{A}_4^{(m)}\right) \times e^{\pm k\eta_{(m)}h}C_{(m)}=0, \tag{3.4a}$$

$$\sum_{m=1}^{8}\left(c_{16}i\overline{A}_1^{(m)}+c_{26}\eta_{(m)}\overline{A}_2^{(m)}+c_{46}\eta_{(m)}\overline{A}_3^{(m)}+c_{56}i\overline{A}_3^{(m)}+c_{66}\eta_{(m)}\overline{A}_1^{(m)}+c_{66}i\overline{A}_2^{(m)}+e_{16}i\overline{A}_4^{(m)}+e_{26}\eta_{(m)}\overline{A}_4^{(m)}\right) \times e^{\pm k\eta_{(m)}h}C_{(m)}=0, \tag{3.4b}$$

$$\sum_{m=1}^{8}\left(c_{14}\mathrm{i}\overline{A}_1^{(m)}+c_{24}\eta_{(m)}\overline{A}_2^{(m)}+c_{44}\eta_{(m)}\overline{A}_3^{(m)}+c_{45}\mathrm{i}\overline{A}_3^{(m)}+c_{46}\eta_{(m)}\overline{A}_1^{(m)}+c_{46}\mathrm{i}\overline{A}_2^{(m)}+e_{14}\mathrm{i}\overline{A}_4^{(m)}+e_{24}\eta_{(m)}\overline{A}_4^{(m)}\right)\times \mathrm{e}^{\pm k\eta_{(m)}h}C_{(m)}=0, \tag{3.4c}$$

$$\sum_{m=1}^{8}\left(e_{21}\mathrm{i}\overline{A}_1^{(m)}+e_{22}\eta_{(m)}\overline{A}_2^{(m)}+e_{24}\eta_{(m)}\overline{A}_3^{(m)}+e_{25}\mathrm{i}\overline{A}_3^{(m)}+e_{26}\eta_{(m)}\overline{A}_1^{(m)}+e_{26}\mathrm{i}\overline{A}_2^{(m)}-\varepsilon_{12}\mathrm{i}\overline{A}_4^{(m)}-\varepsilon_{22}\eta_{(m)}\overline{A}_4^{(m)}\right)\times \mathrm{e}^{\pm k\eta_{(m)}h}C_{(m)}=0. \tag{3.4d}$$

If (2.3) is used instead of (2.4) and (3.4d) should be replaced by

$$\sum_{j=1}^{8}\overline{A}_4^{(m)}\mathrm{e}^{\pm k\eta_{(m)}h}C_{(m)}=0. \tag{3.5}$$

For nontrivial solutions of $C_{(m)}$, the determinant of the coefficient matrix of (3.4a)–(3.4d) has to vanish, and this leads to the frequency equation that determines the wave speed. We note that the eigenvalue problem for ω represented by (3.4a)–(3.4d) is for an unbounded plate. A basic feature of an eigenvalue problem over an unbounded domain is that it usually has a continuous spectrum. That is, any value of ω is an eigenvalue for which there exist waves with corresponding wavelengths. This is fundamentally different from the case of pure thickness waves in which, although the plate itself is unbounded, the eigenvalue problem is in fact defined over a finite domain, i.e., the plate thickness, and has a discrete spectrum.

We turn now to solve the eigenvalue problem (3.4a)–(3.4d) for frequency ω using a iterative numerical procedure. For a given real value of k, we choose a real trial value of ω, and with this pair of known tentative values of ω and k, we determine the eigenvalues—the eight roots $\eta_{(m)}$ of the polynomial equation of η, and the corresponding eigenvectors $\left(\overline{A}_j^{(m)},\overline{A}_4^{(m)}\right)$ from (3.2). Substituting the so-determined $\eta_{(m)}$ and $\left(\overline{A}_j^{(m)},\overline{A}_4^{(m)}\right)$ into the determinant of the coefficient matrix of (3.4a)–(3.4d) results in a formally complex determinant, or equivalently two real determinants (the real and imaginary parts of the complex determinant). Our numerical analysis shows that one of the two real determinants is always so small that it cannot be well captured within the machine precision and thus it should be treated as zero numerically. If the above trial ω cannot make the remaining determinant vanish, we choose another trial value of ω to pair the same k and we repeat the above procedure until the remaining determinant vanishes. The so-determined ω together with the given k defines a point on the dispersion curve in the k–ω plane, and through this procedure, we obtain a dispersion relation in the form of $\omega=\omega(k)$, from which the phase velocity and group velocity of the waves can be determined. One can expect that this dispersion relation have many branches, analogous to the waves propagating in an elastic plate. We note the fact that a real ω makes a formally complex determinant (which in fact should be either real or pure imaginary because one of the two real determinants is always numerically zero) vanish is consistent with what was previously observed in the special cases discussed in Mindlin (1984) and Onoe et al. (1963), where an analytical approach can be carried to the end, resulting in a real (or pure imaginary) determinant.

We recognize that the present discussion concerns with idealized materials without lossy mechanisms and consequently, the waves propagate without attenuation. For lossy materials, a genuine complex wave number is required to satisfy the complex frequency equation because of attenuation.

4. Numerical results and discussion

As a numerical example, we consider polarized ceramics PZT-5H for which we have, when the poling direction is along the x_3 axis (Auld, 1973)

$$
\begin{aligned}
&c_{11} = 12.6, \quad c_{33} = 11.7, \quad c_{44} = 2.30,\\
&c_{12} = 7.95, \quad c_{13} = 8.41 \times 10^{10}\ \mathrm{N/m^2}, \quad c_{66} = (c_{11} - c_{12})/2,\\
&e_{15} = 17.0, \quad e_{31} = -6.5, \quad e_{33} = 23.3\ \mathrm{C/m^2},\\
&\varepsilon_{11} = 1700\varepsilon_0, \quad \varepsilon_{33} = 1470\varepsilon_0, \quad \varepsilon_0 = 8.854 \times 10^{-12}\ \mathrm{F/m}.
\end{aligned}
\tag{4.1}
$$

The material constants for PZT-5H poled in any other directions can be determined by tensor transformation.

As a special case, we first determine the dispersion relations for a nonrotating plate ($\Omega = 0$) with the poling direction along the x_3 axis. In this case, u_1 is coupled with u_2, and u_3 is coupled with ϕ, but the two groups do not couple each other. The dispersion relations for this case had been previously obtained analytically in a close-form (Tiersten, 1963a,b; Bleustein, 1969). A comparison of the dispersion relations generated by our computer code with the close-form solutions shows that the two are indeed identical. This serves as a precaution measure for verification of our general formulation and the solution procedure. There exist infinite number of branches of dispersion relations. The first nine branches are shown in Fig. 2 for a plate with a pair of shorted electrodes using the boundary conditions (2.3), and in Fig. 3 for an unelectroded plate using the boundary conditions (2.4). In Figs. 2 and 3, the wave frequencies are normalized by the lowest thickness-shear frequency of an isotropic elastic plate with shear modulus c_{44}

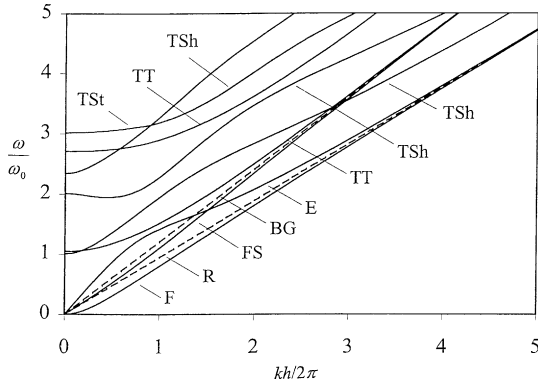

Fig. 2. Dispersion relations of an electroded ceramic plate poled along the x_3 direction ($\Omega = 0$).

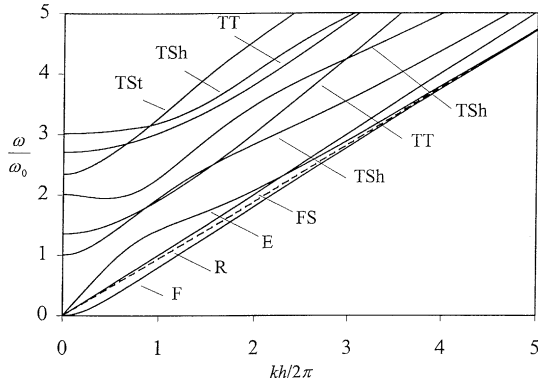

Fig. 3. Dispersion relations of an unelectroded ceramic plate poled along the x_3 direction ($\Omega = 0$).

$$\omega_0 = \frac{\pi}{2h}\sqrt{\frac{c_{44}}{\rho}}. \tag{4.2}$$

The dispersion relations are labeled according to Mindlin (1984), along with the dominant displacement component at small wave numbers, as follows:

E	extension (u_1),
F	flexure (u_2),
FS	face-shear (u_3),
TSh	thickness-shear (u_1),
TSt	thickness-stretch (u_2),
TT	thickness-twist (u_3),
R	Rayleigh surface wave (u_1 and u_2),
BG	Bleustein–Gulyaev surface wave (u_3).

In Fig. 2, the three branches intercepting the origin are the so-called low frequency branches. They represent the extensional, flexural, and face-shear waves. The other six branches are high-frequency branches all of which have finite intercepts with the ω axis. These intercepts are called cut-off frequencies, below which the corresponding waves cannot propagate. Cut-off frequencies are in fact the frequencies of pure thickness waves, which are the main result of Bleustein (1968) and a special case of the present study. The six high frequency branches shown in the figures represent three thickness-shear waves, one thickness-stretch wave, and two thickness-twist waves. One of the two dotted lines in Fig. 2 is the frequency-wave number relation for the well-known Rayleigh surface wave, which can propagate over an elastic half-space and is not dispersive. The other dotted line is the frequency-wave number relation for the Bleustein–Gulyaev surface wave, which has only one displacement component u_3 and can propagate over an piezoelectric half-space but does not have an elastic counterpart (Bleustein, 1968; Gulyaev, 1969; Lothe and Barnett, 1976). It is seen from Fig. 2 that for short waves with larger k, the frequencies of the extensional and flexural waves approach that of the Rayleigh surface wave, and we note that the corresponding waves in elastic plates have the same feature (Eringen and Suhubi, 1975). Similarly, for short waves, the frequency of the lowest thickness-twist wave approaches that of the Bleustein–Gulyaev wave, and we note that both the waves are associated with the same displacement component u_3.

For the case of an unelectroded plate, the corresponding Bleustein–Gulyaev wave in a half-space requires the inclusion of the free space electric field, which is excluded by the boundary condition $D_2(\pm h) = 0$ considered here. Therefore the corresponding Bleustein–Gulyaev wave does not exist in the present case, and the single dotted line in Fig. 3 represents the Rayleigh wave. The second difference between Figs. 2 and 3 is that the thickness-twist waves in Fig. 3 have slightly higher frequencies than the corresponding waves in Fig. 2. This is because thickness-twist waves are electrically coupled. When the plate is electroded, the electric field components E_1 and E_3 have to vanish on the electrodes. Furthermore, when the electrodes are shorted, the average of the electric field component E_2 along the plate thickness has to be zero. The electric field within a plate with two shorted electrodes on its major surfaces is therefore confined to certain degree. The related piezoelectric stiffening effect due to electric fields, though small, tends to raise the resonant frequencies. For materials of strong piezoelectric coupling such as polarized ceramics, the electrical boundary conditions can influence the resonant frequencies through the distribution of the electric field in the body and the related piezoelectric stiffening effect.

The effect of rotation on the dispersion relations, especially the branches representing the lowest thickness-shear and the lowest thickness-twist waves, are of particular interest for gyroscope applications. We thus plot the rotation-induced shifts of frequencies of the lowest thickness-shear and thickness-twist waves in Fig. 4 for a ceramic plate poled along the x_2 direction with shorted electrodes and in Fig. 5 for the

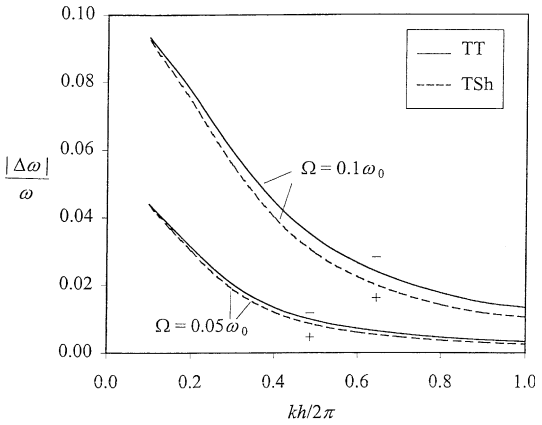

Fig. 4. Rotation-induced frequency shift for the lowest thickness-shear and thickness-twist waves versus the wave number, for an electroded ceramic plate poled long its normal direction.

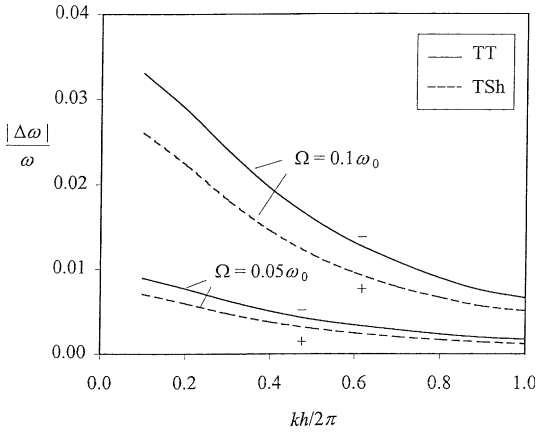

Fig. 5. Rotation-induced frequency shift for the lowest thickness-shear and thickness-twist waves versus the wave number, for an unelectroded ceramic plate poled long its normal direction.

corresponding unelectroded plate, respectively. The numerical results are plotted for $0.1 < kh/2\pi < 1$, because long waves with $\lambda = 2\pi/k \gg h$ or $kh/2\pi \ll 1$ are usually used for plate-like piezoelectric devices working with thickness-shear modes (Reese et al., 1989; Yang et al., 1988; Abe et al., 1998). The frequency shift is defined by $\Delta\omega = \omega(\Omega) - \omega(0)$. In these figures, the relative frequency shifts $|\Delta\omega/\omega|$ are plotted, with plus and minus signs indicating upward and downward shifts, respectively. Our analysis shows that the frequency shifts increase monotonically with the rotation rate Ω when Ω is much smaller than the lowest thickness-shear resonance frequency of the plate (approximately equal to ω_0), which is realistic for gyroscope applications. It is seen from Figs. 4 and 5 that the frequency shifts are relatively large for small wave numbers, corresponding to long waves, and the frequency shifts diminish as the wave number k becomes increasingly large. This indicates that long waves are more sensitive to rotation than short waves. We note from Figs. 4 and 5 that the electroded plate has significantly larger frequency shifts than the unelectroded plate, indicating the electroded plate has a higher rotation sensitivity for the wave modes considered. In fact, our analysis shows that this feature remains true for ceramic plates poled along the x_1 axis, or the x_3

axis, or along a direction bisecting the angle between the x_1 and x_3 axes. The corresponding numerical results are not shown here because there are no characteristic differences from those shown in Figs. 4 and 5. What has caught our particular attention is the observation that the frequency shifts do not decrease monotonically with the increasing wave number for unelectroded plates poled along the x_3 axis. Instead, the frequency shift for each of these modes rises with the wave number initially, reaching a maximum before it diminish as the wave number becomes increasingly large, as seen in Fig. 6. We note that this maximum is of particular interest for development of rotation sensors.

We plot in Figs. 7 and 8 for electroded and unelectroded plates, respectively, the shift of frequencies of the lowest thickness-shear and thickness-twist waves versus the rotation rate, for a fixed wave number: $kh/2\pi = 0.1$, representing reasonably long waves. The frequency shift increases with the rotation rate monotonically in all the cases, which is desirable for rotation sensor applications. It is also evident from Figs. 7 and 8 that the frequency shifts are substantially larger for plates poled along the x_3 axis than for the plates poled along the x_1 axis, indicating greater rotation sensitivity. What is more important is the fact that the curves in Fig. 7 both have finite initial slopes, indicating an initially linear relation between the rotation rate and the frequency shift, which is particularly desirable for sensor applications. For the curves in Fig. 8,

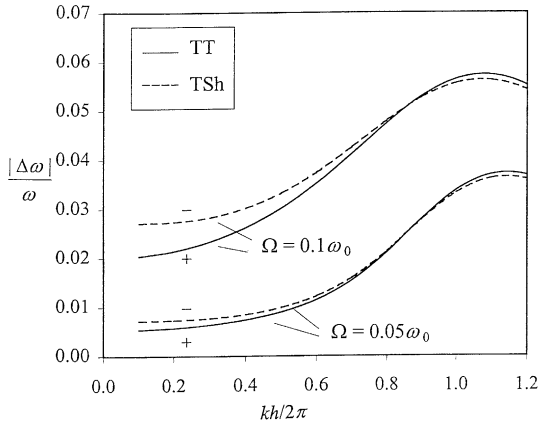

Fig. 6. Rotation-induced frequency shift for the lowest thickness-shear and thickness-twist waves versus the wave number, for an unelectroded ceramic plate poled long the x_3 direction.

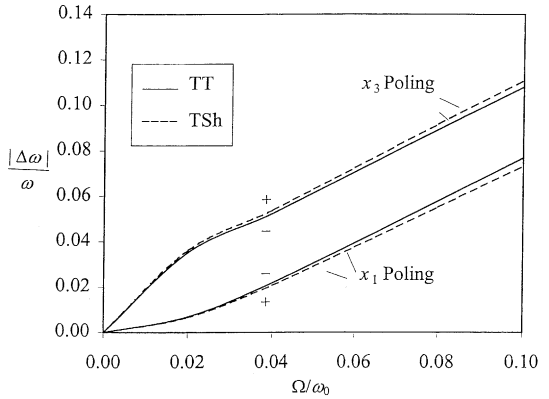

Fig. 7. Rotation-induced frequency shift for the lowest thickness-shear and thickness-twist waves versus the rotation rate, for an electroded ceramic plate ($kh/2\pi = 0.1$).

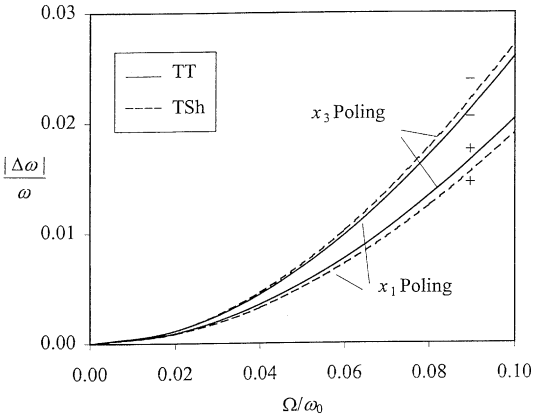

Fig. 8. Rotation-induced frequency shift for the lowest thickness-shear and thickness-twist waves versus the rotation rate, for an unelectroded ceramic plate ($kh/2\pi = 0.1$).

the tangents at the origin appear to be essentially flat, suggesting that they should be avoided in rotation sensor applications if frequency shifts are to be measured. However, this type of behavior is desirable for applications in which a resonant frequency *insensitive* to rotation is required. In a previous study (Fang et al., 2000), we have shown that the wave frequency may shift with rotation rate linearly or quadratically, depending upon the material poling direction versus the rotation axis. In the present case where long waves propagate within a piezoelectric plate, this characteristic of the frequency shift depends also upon the electric boundary conditions on the major faces of the plate.

5. Conclusion

The characteristics of the dispersion relations of waves propagating in a polarized ceramic plate rotating about its normal at a constant rate are presented. The rotation sensitivity is analyzed in details for the lowest thickness-shear and the lowest thickness-twist waves because of the particular importance of these modes for gyroscope applications. The frequency shifts monotonically with the increasing rotation rate and the rotation sensitivity of long waves is substantially greater than that of short waves. Generally, plates with shorted electrode surfaces have higher rotation sensitivity than plates with free-charge surfaces. For long waves and for small rotation rate relative to the wave frequency, the frequency shifts with rotation rate, linearly for plates with shorted electrode surfaces and nonlinearly with a nearly flat initial tangent for plates with free-charge surfaces. These rotation sensitivity characteristics are of interest for the development of rotation sensors and other piezoelectric devices for which frequency insensitivity to rotation is desired.

Acknowledgement

This work is supported by the Office of Naval Research under contract number ONR N00014-96-1-0884.

References

Abe, H., Yoshida, T., Watanabe, H., 1998. Energy trapping of thickness-shear vibrations excited by parallel electric field and its applications to piezoelectric vibratory gyroscopes. In: Proceedings of IEEE International Ultrasonics Symposium, pp. 467–471.

Auld, B.A., 1973. In: Acoustic Fields and Waves in Solids, vol. 1. John Wiley & Sons, New York, pp. 357–382.

Bleustein, J.L., 1968. A new surface wave in piezoelectric materials. Applied Physics Letters 13, 412–413.
Bleustein, J.L., 1969. Some simple modes of wave propagation in an infinite piezoelectric plate. Journal of Acoustical Society of American 45, 614–620.
Clarke, N.S., Burdess, J.S., 1994. A rotation rate sensor based upon a Rayleigh resonator. ASME Journal of Applied Mechanics 61, 139–143.
Eringen, A.C., Suhubi, E.S., 1975. In: Elastodynamics, vol. II. Academic Press, New York.
Fang, H.Y., Yang, J.S., Jiang, Q., 2000. Rotation-perturbed surface acoustic waves propagating in piezoelectric crystals. International Journal of Solids and Structures 37, 4933–4947.
Gulyaev, Yu.V., 1969. Electroacoustic surface waves in solids. Soviet Physics JETP Letters 9, 37–38.
Lao, B.Y., 1980. Gyroscopic effect in surface acoustic waves. In: Proceedings of IEEE Ultrasonics Symposium, pp. 687–691.
Lothe, J., Barnett, D.M., 1976. Integral formulism for surface waves in piezoelectric crystals: existence considerations. Journal of Applied Physics 47, 1799–1807.
Mindlin, R.D., 1984. Frequencies of piezoelectrically forced vibrations of electroded, doubly rotated, quartz plates. International Journal of Solids and Structures 20, 141–157.
Onoe, M., Tiersten, H.F., Meitzler, A.H., 1963. Shift in the location of resonant frequencies caused by large electromechanical coupling in thickness-mode resonators. Journal of Acoustical Society of American 35, 36–42.
Paul, H.S., 1968. Vibrational waves in a thick infinite plate of piezoelectric crystal. Journal of Acoustical Society of American 44, 478–482.
Paul, H.S., Raman, K.G.V., 1991. Vibrations of pyroelectric plates. Journal of Acoustical Society of American 90, 1729–1732.
Paul, H.S., Renganathan, K., 1985. Free vibrations of a pyroelectric layer of hexagonal (6 mm) class. Journal of Acoustical Society of American 78, 395–397.
Paul, H.S., Raju, D.P., Balakrishnan, T.R., 1983. Free vibrations of a piezoelectric layer of hexagonal (6 mm) class. International Journal of Engineering Science 21, 691–704.
Reese, G.M., Marek, E.L., Lobitz, D.W., 1989. Three-dimensional finite element calculations of an experimental quartz resonator sensor. In: Proceedings of IEEE Ultrasonics Symposium, pp. 419–422.
Schmidt, G.H., 1977a. On anti-symmetric waves in an unbounded piezoelectric plate with axisymmetric electrodes. International Journal of Solids and Structures 13, 179–195.
Schmidt, G.H., 1977b. Resonances of an unbounded piezoelectric plate with circular electrodes. International Journal of Engineering Science 15, 495–510.
Shick, D.V., Zhou, Y.S., Tiersten, H.F., 1989. Analysis of the in-plane acceleration sensitivity of quartz surface wave resonators rigidly supported along the edges. Journal of Applied Physics 65, 35–41.
Stewart, J.T., Yong, Y.K., 1994. Exact analysis of the propagation of acoustic waves in multilayered anisotropic piezoelectric plates. IEEE Transactions on Ultrasonics, Ferroelectrics, and Frequency Control 40, 375–390.
Syngellakis, S., Lee, P.C.Y., 1993. Piezoelectric wave dispersion curves for infinite anisotropic plates. Journal of Applied Physics 73, 7152–7161.
Tiersten, H.F., 1963a. Thickness vibrations of piezoelectric plates. Journal of Acoustical Society of American 35, 53–58.
Tiersten, H.F., 1963b. Wave propagation in an infinite piezoelectric plate. Journal of Acoustical Society of American 35, 234–239.
Tiersten, H.F., 1969. Linear Piezoelectric Plate Vibrations. Plenum, New York.
Tiersten, H.F., Shick, D.V., 1988. On the normal acceleration sensitivity of SC-cut quartz surface wave resonators supported along rectangular edges. Journal of Applied Physics 64, 4334–4341.
Tiersten, H.F., Stevens, D.S., Das, P.K., 1980. Acoustic surface wave accelerometer and rotation rate sensor. In: Proceedings of IEEE Ultrasonics Symposium, pp. 692–695.
Tiersten, H.F., Stevens, D.S., Das, P.K., 1981. Circulating flexural wave rotation rate sensor. In: Proceedings of IEEE Ultrasonics Symposium, pp. 163–166.
White, R.W., 1998. Acoustic sensors for physical, chemical and biochemical applications. In: Proceedings of IEEE International Frequency Control Symposium, pp. 587–594.
Yang, J.S., Fang, H., Jiang, Q., 1988. Thickness vibrations of rotating piezoelectric plates. Journal of Acoustical Society of American 104, 1427–1435.